Experimental Study on Reinforced Concrete Walls with High Axial Loads

A.V. Shegay, C.J. Motter, R.S. Henry & K.J. Elwood

Department of Civil and Environmental Engineering, University of Auckland, Auckland.

2017 NZSEE Conference

ABSTRACT: Following the 2010/2011 Canterbury Earthquakes in New Zealand, unexpected failure modes were observed in reinforced concrete (RC) structural walls, despite being designed to ductile provisions of the New Zealand Concrete Structures Standard (NZS3101:2006). These observations have raised concern on the reliability of the current design provisions in ensuring a ductile wall response in an earthquake event. A key aspect that can influence the response of RC walls in earthquakes is the imposed axial load. Excessive axial loads can diminish yielding of reinforcement, and therefore energy dissipation capacity, leading to brittle compressive failure. Amendments have been proposed to NZS3101:2006 to address the unexpected failure modes in walls by limiting the wall axial load to $0.3A_g f'_c$. To investigate the effects of axial load on wall performance, quasi-static tests have been conducted on three large-scale rectangular RC walls. Test results indicated that walls designed to the proposed amended standard and low axial loads ($N = 0.09A_g f'_{c.test}$) have a ductile response as intended, with concrete damage limited to flexural cracking and end region concrete cover spalling up to 2.0% drift and failure occurring at 3.19% drift. At higher axial loads of $0.2A_g f'_{c.test}$, drift capacity reduced significantly to 2.06% and the failure mode became considerably more brittle. Extrapolation of these results was used to approximate that at the new proposed limit of $0.3A_g f'_c$, the drift capacity is 1.4%.

1 INTRODUCTION

Extensive research into the performance of reinforced concrete (RC) walls began in the 1970s, and since then, numerous studies have demonstrated that RC walls are stiff components that can sustain large drift demands and provide ductility and energy dissipation when subjected to lateral loading. However, observed damage from the 2010/2011 Canterbury, New Zealand Earthquakes and the 2010 Maule Earthquake in Chile has indicated that, although most reinforced concrete wall buildings achieved their life-safety design objective, a number of RC walls sustained severe and unexpected damage. The observed damage included crushing of concrete in compression (**Figure 1a**), vertical reinforcement buckling (**Figure 1b**), and in some cases global out-of-plane buckling of the section (**Figure 1c**).

A major factor that can contribute to the above failures is the axial load carried by the wall. Axial load increases the stresses experienced in the end region of the wall which can cause a premature and brittle compressive failure mode. In New Zealand and the United States of America, the concrete structural standards, NZS3101:2006 (Standards New Zealand, 2012) and ACI-318-14 (ACI Committee 318, 2014), respectively, currently do not limit the axial load that can be attributed to a wall. The Chilean structural standard (DS 60 MINVU, 2010) had introduced an axial load limit of $0.35A_g f'_c$, where Ag is the gross cross-sectional area of the wall and f'_c is the specified compressive strength of concrete. For New Zealand mid- to high-rise construction, typical axial loads range from 0.05-0.15 $A_g f'_c$ (Bull, 2016; Stevenson et al, 2015; Yong, 2016), while in Chilean construction the range is between 0.2-0.4 $A_g f'_c$ (Massone et al., 2012), and can increase by up to 50% when earthquake loads are considered (Alarcon et al, 2014). Additionally, the axial load on a wall may be further increased through interaction between structural elements, such as wall elongation restraint from floor diaphragms tying into the wall or coupling beams action (Yoshimura et al, 1985).

(a) **(b)** **(c)**

Figure 1: (a) Axial crushing failure of main load bearing wall, Christchurch (courtesy of Dunning Thornton Consulting), (b) crushing and reinforcement buckling of wall end region, Chile (Wallace, 2011), (c) out-of-plane buckling and crushing of perimeter wall, Christchurch (courtesy of Rick Henry).

Reinforced concrete wall failure in the The Grand Chancellor Hotel (**Figure 1a**) was analysed by two independent engineering consultants with results reported in Volume 2 of the Canterbury Earthquakes Royal Commission report (CERC 2012). The report identifies large axial load to be a major factor in contributing to the failure of this wall. As a response to this, an axial load limit of $0.3A_g f'_c$ has been proposed to the third amendment (A3) of NZS3101:2006 which is currently its public comment stage (Standards New Zealand, 2015). This limit was developed largely based on engineering judgement rather than research, which has prompted the experimental investigation described in this paper in order to assess the suitability of this limit.

1.1 Recent study on effects of axial loads

Alarcon (2013) investigated the effects of axial load on unconfined walls typically designed in Chile by testing three specimens with axial loads of 0.15, 0.25 and $0.35A_g f'_c$ (W1, W2 and W3, respectively). All three walls had an identical rectangular 700 × 100mm cross-section (length to thickness ratio of 7), as shown in **Figure 2a**. Typical observed damage at the end of the test is also shown in **Figure 2a**. The hysteretic response of these specimens is presented in **Figure 2b** below. All three walls failed in axial-flexural compression. Significant deterioration in drift capacity as axial load increases is evident in the results. Peak drift capacity (drift at failure) was 2.8%, 1.8%, and 1.5% for W1 ($0.15A_g f'_c$), W2 ($0.25A_g f'_c$), and W3 ($0.35A_g f'_c$), respectively. The results also show that failure becomes more brittle as axial load increases; noting that failure in W2 and W3 occurred almost immediately after peak strength was reached as seen in **Figure 2b**. The compression failure was followed by significant movement of the entire wall cross-section in the out-of-plane direction along a diagonal plane indicating significant axial load contribution to the failure mode similar to that shown in **Figure 2a**. The author concluded that the proposed limit of $0.35A_g f'_c$ in the new Chilean concrete structures code (DS 60 MINVU, 2010) is inadequate in preventing brittle wall failures in post-1985, Chilean high-rise wall construction, characterised by no or limited end region confinement.

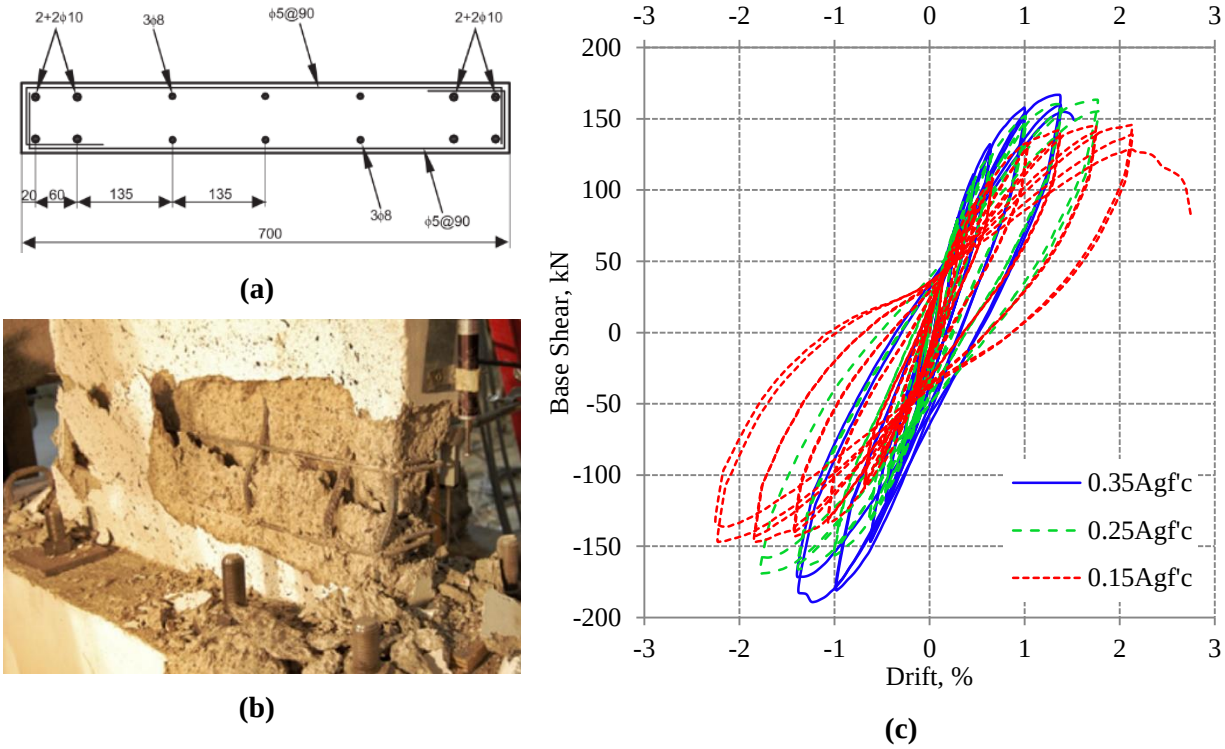

Figure 2: (a) cross-section used for W1-W3 (at top left) , (b) typical observed damage at failure (at bottom left), (c) base shear versus drift plots for W1-W3 (at right) (C. N. O. Alarcon, 2013)**.**

2 NZS3101 AMENDMENT TESTING PROGRAMME

The test specimens discussed in the preceding section are not representative of typical construction and detailing used in New Zealand for 'ductile' class walls. The major differences include geometry (typical wall length to thickness ratio in New Zealand is above 10 (Stevenson et al., 2015)) and end region confinement detailing. To investigate the effects of axial load on typical New Zealand ductile RC walls, three one-half-scale test specimens were designed to NZS3101:2006(A3) and tested. The cross-sections for the specimens (A09, A14 and A20) are presented in **Figure 3**, with key test variables and parameters summarised in **Table 1**. In **Table 1**, f'_c refers to the specified compressive strength of concrete and $f'_{c.test}$ refers to the compressive strength of concrete measured from 100 x 200mm cylinder tests on the day of the experiment. The testing set up is presented in **Figure 4**. Specimens are identified by the percent axial load applied (e.g. 'A20' refers to a wall designed to the proposed Amendment 3 subjected to $0.2A_g f'_c$). The cross-section for all three specimens is 2250 mm (length) by 200 mm (thickness) which corresponds to a length to thickness ratio of 11.25. The longitudinal reinforcement layout is identical for the three specimens. Self-compacting concrete with f'_c = 30MPa was used in constructing the walls to allow adequate compaction between the reinforcement; this would not typically be necessary in a full-scale wall.

For each specimen, asymmetric end region detailing was used to compare the effectiveness of confinement provided by hoops to that provided by cross-ties. Grade 500E (f_y = 500Mpa) was used for the longitudinal and shear reinforcement throughout the wall, and a mix of Grade 300E (f_y = 300Mpa) and Grade 500E smooth bars were used for confinement reinforcement as shown in **Figure 3**. The walls have been designed for demands of an 8-storey idealized prototype building located in Wellington, New Zealand. To ensure a flexural response, capacity design principles were adopted for shear strength design, resulting in low shear demands ranging from 0.15-0.19$\sqrt{f'c}$ (MPa) as shown in **Table 1**. Only the bottom two storeys of the idealized prototype were constructed for testing, resulting in a total wall clear height of 3.5 m. To compensate for the specimen size, a base moment to base shear ratio of 10.35 was maintained throughout the test.

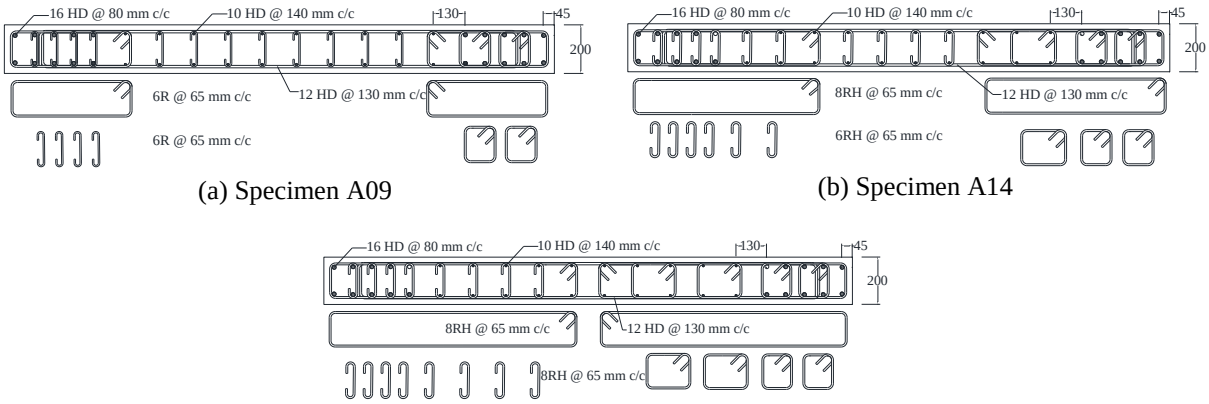

(a) Specimen A09

(b) Specimen A14

(d) Specimen A20

Note: 25mm clear concrete cover all around was used.

Figure 3: Cross-sections of wall specimens

Table 1: Key specimen design variables and parameters

Specimen	Axial load (f'_c)*	Axial load ($f'_{c.test}$)*	M_n*, kNm	Shear stress demand, $V@M_n/A_g\sqrt{f'_c}$, MPa
A09	$0.1A_gf'_c$	$0.09A_gf'_{c.test}$	3738	0.15
A14	$0.2A_gf'_c$	$0.14A_gf'_{c.test}$	4497	0.18
A20	$0.3A_gf'_c$	$0.20A_gf'_{c.test}$	4955	0.19

* $f'_{c.test}$ is the average measured concrete cylinder strength on the day of specimen testing.

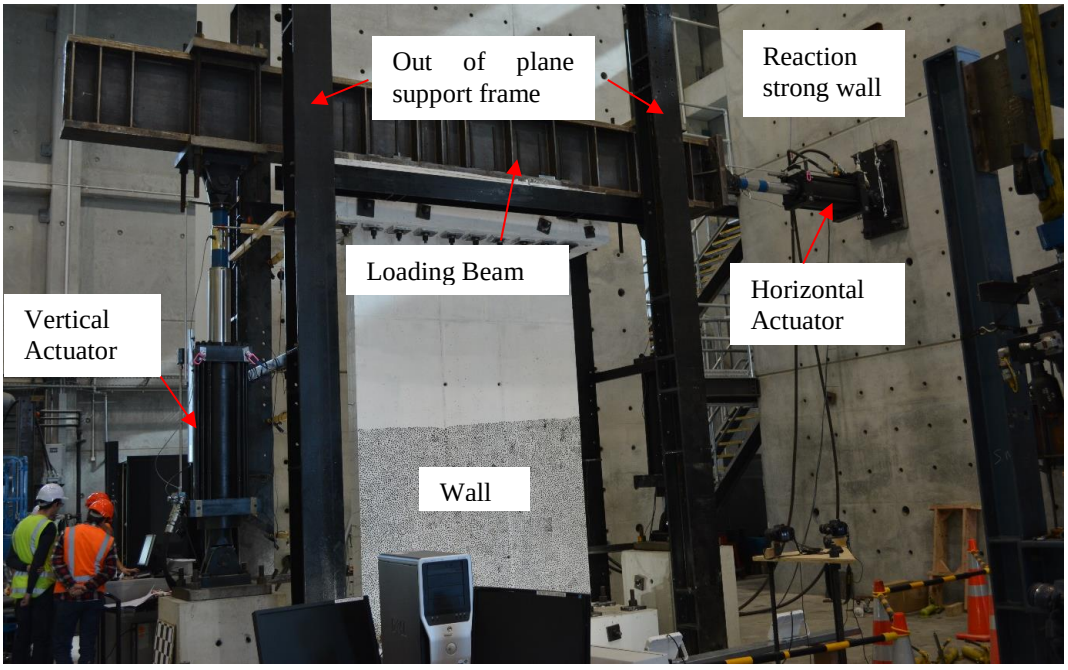

Figure 4: Photo of experimental set up.

3 EXPERIMENTAL RESULTS

The normalized base-moment versus drift hysteresis plots are presented in **Figure 5a-d**. A summary of key results is shown in **Table 2**.

3.1 **Load-deformation**

It is observed from Figure 5: Base-moment versus drift hysteresis plots for A09, A14 and A20.**Figure 5** and **Table 2: Summary of key results for walls A09, A14 and A20.** that an increase in axial load ratio resulted in a corresponding increase in peak base moment and peak base shear in the walls. The strength increased 17% with a 56% increase in axial load for A14 relative to A09 and by 15% with a 43% increase in axial load for A20 relative to A14. On average, the peak base moment had exceeded the nominal base moment (calculated using measured material properties and using assumption outlined in NZS3101:2006) by a factor of 1.14. Conversely, the maximum attained drift decreased with increasing axial load. A drift of 3.19% was achieved by specimen A09 before failure occurred, and this drift capacity would exceed the peak demands experienced by most buildings in earthquakes. Comparatively, the drift capacity for specimens A14 and A20 relative to A09 decreased by 18% and 35% (corresponding to 2.62% and 2.06% maximum drift, as shown in **Table 2**), respectively, due to the effects of increased axial load.

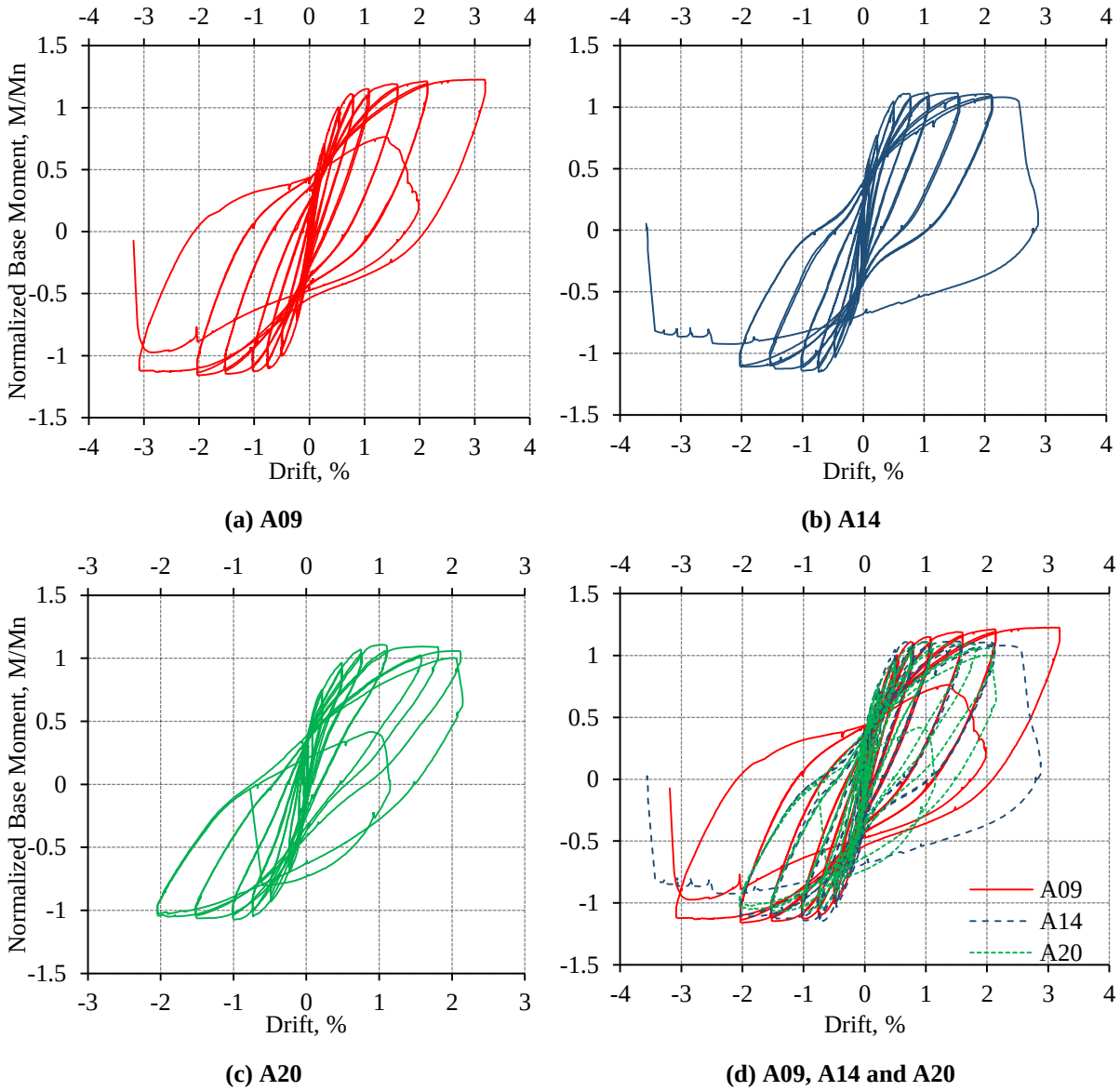

Figure 5: Base-moment versus drift hysteresis plots for A09, A14 and A20.

Table 2: Summary of key results for walls A09, A14 and A20.

Specimen	V_{max} [(1)], kN		M_{max} [(1)], kNm		M_{max}/M_n [(1)]		Δ_{ult} [(2)], %	
	Pos.	*Neg.*	*Pos.*	*Neg.*	*Pos.*	*Neg.*	*Pos.*	*Neg.*
A09	456	-431	4655	-4401	1.23	-1.16	3.19	-3.05
A14	554	-555	5438	-5601	1.12	-1.15	2.62	-2.46
A20	673	-675	6252	-6056	1.11	-1.07	2.06	-2.05

[(1)] V_{max}, M_{max} and M_n are the peak base shear, peak base moment and nominal base moment (calculated used measured material properties), respectively.
[(2)] Δ_{ult} is the ultimate drift capacity defined as the point at which the base moment drops to 80% of M_p.

3.2 General damage

Throughout the tests, all walls exhibited a well-distributed cracking pattern over the entire height of the wall. The crack spacing was consistent across all tests and approximately equivalent to the spacing of the transverse confinement reinforcement (65mm). The majority of the cracks were horizontal in orientation, particularly at smaller drift cycles (<0.75%), and became more inclined in high drift cycles (>0.75%). Spalling of cover concrete initiated at 1.0% drift for specimens A09 and A14 and at 0.75% drift for A20. Throughout the tests, the extent of spalling increased up the height of the wall (up to around 1200mm from the base of the wall for all specimens). Spalling of cover concrete had also increased into the web of the wall with higher axial load (200mm, 500mm and 850mm for A09, A14 and A20, respectively), reflecting the deeper compression zone required to maintain section equilibrium.

3.3 Failure mode

Specimen A09 had sustained a full cycle at 3.0% drift. On the reverse cycle to -3.0%, the two outermost longitudinal bars at the compressive end region buckled at a height of 600mm above the base of the wall, occurring over four confinement hoops. The reinforcement in both curtains buckled in the same direction. The confined concrete core of the end region remained in-plane without crushing, and buckling of longitudinal reinforcement was not observed in any other longitudinal bars. Upon unloading from -3.0% drift, reinforcement buckling was observed on the opposite end of the wall, occurring over eight transverse hoops, as shown in **Figure 6a**. In this case, the confined core of the wall participated in the buckling mode resulting in global out-of-plane movement and associated gradual loss in capacity seen in **Figure 5a**. The resulting failure was very similar to that observed in the Pacific Tower office building after the 22 February Christchurch earthquake previously shown in **Figure 1c**. The failure is considered to be a tension-governed mechanism initiated by large tensile strain of the longitudinal reinforcement (Rodriguez et al. 1999).

Comparatively, both specimens A14 and A20 failed in pure compression by crushing of the confined end region core. The deterioration of the core in specimen A14 resulted in large axial movement of the end region, causing longitudinal reinforcement to buckle. Buckling of longitudinal reinforcement in this failure mode was observed to be highly localized, in some areas occurring over a length of one hoop spacing as shown in **Figure 6b**. Concrete core crushing was similarly observed to be highly localized, occurring over 2 to 3 hoops spacing intervals (130 - 200mm). For specimen A20, the large axial deformations resulting from the deterioration of the core resulted in some noticeable out of plane movement of the end region (**Figure 6c)** prior to complete loss of capacity through localised crushing. Unlike specimen A14, A20 failed on a repeat cycle (at 2.0% drift), suggesting cyclic degradation was a contributing factor to the failure mode.

(a) (b) (c)

Figure 6: (a) Out-of-plane buckling of the end region in wall A09, (b) compression failure resulting in highly localized reinforcement buckling in wall A14 (c) compression failure resulting in out-of-plane movement of the end region in wall A20.

In an attempt to crudely estimate the drift capacity of an RC wall tested at an axial load of $0.3A_g f'_c$, a trend line (shown as red dash) was fit to the available drift capacity data from the completed tests, as shown in **Figure 7** below, with an estimated drift of 1.42%. This value is less than half of the aforementioned permissible 3.6% drift limit. Results from the tests conducted on specimens W1-W3 by Alarcon et al. (2014) are also plotted in **Figure 7** for comparison to the test specimens. There is reasonable agreement between the two studies presented, despite a significant difference in the level of confinement provided at the wall end region. The smaller length to thickness ratio for W1-W3 (l_w/t_w = 7) is likely having a beneficial effect on the drift capacity, consistent with previous research (Whitman, 2015).

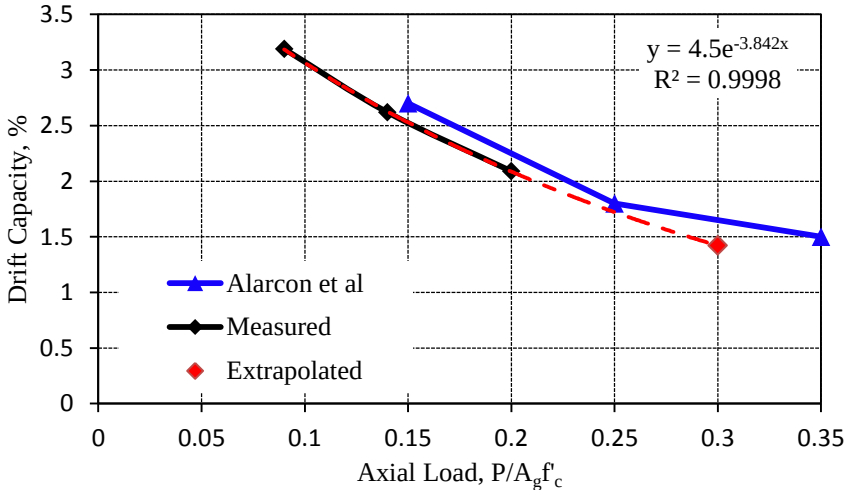

Figure 7: Extrapolating available experimental data to predicting drift capacity at higher axial loads.

4 SUMMARY

The proposed NZS3101:2006(A3) recommended limit of $0.3A_g f'_c$ on the axial load for reinforced concrete walls has been investigated in an experimental study on three one-half-scale specimens designed and detailed to the 'ductile' class under NZS3101:2006. Specimen A09, subjected to an axial load of 0.09 $A_g f'_c$, sustained one full cycle at a maximum lateral drift of 3.19% prior to instability and

failure during the second cycle at this level. Damage to this specimen was characterized by well distributed spalling of concrete cover, yielding of reinforcement and eventual failure in a tension governed mechanism (out-of-plane instability of the end region). Increasing the axial load to 0.14 $A_g f'_c$ in specimen A14 shifted the failure mode to a pure compression-type mechanism, characterized by highly localized crushing occurring in the end region. The drift capacity of A14 was 2.62%, which is 18% less than that of A09. Similarly, specimen A20 had also failed in a pure compression with no prior reinforcement buckling observed prior to concrete crushing. The drift capacity of A20 was 2.06%, which was 35% less than A09. Based on the results of these tests, it is evident that walls with axial loads <0.15 $A_g f'_c$ that are designed to high ductility under the current (and proposed) version of NZS3101:2006 can sustain drift demands in excess of 2% prior to failure. Comparatively, walls tested with high axial loads (>0.20$A_g f'_c$), cannot sustain drift demands beyond 2.0%. Through extrapolation of test results it is estimated that walls designed at the proposed NZS3101:2006(A3) axial load limit of 0.3$A_g f'_c$ will achieve a drift capacity of 1.4%.

5 REFERENCES

ACI Committee 318. (2014). Building Code Requirements for Structural Concrete (ACI 318-14) and Commentary (ACI 318R-14). Michigan, Famington Hills: American Concrete Institute. https://doi.org/10.1016/0262-5075(85)90032-6

Alarcon, C., Hube, M. A., & de la Llera, J. C. (2014). Effect of axial loads in the seismic behavior of reinforced concrete walls with unconfined wall boundaries. *Engineering Structures*, *73*, 13–23. https://doi.org/10.1016/j.engstruct.2014.04.047

Alarcon, C. N. O. (2013). *Influence of Axial Load in the Seismic Behavior of Reinforced Concrete Walls with Nonseismic Detailing*. Pontificia Universidad Catolica De Chile.

Bull, D. K. (2016). Personal communication. Nov. 2015. Auckland, New Zealand.

Canterbury Earthquake Royal Commission. (2012). *Volume 2: The Performance of Christchurch CBD Buildings* (Vol. 2).

DS 60 MINVU. (2010). Reinforced concrete design code, replacing D.S N 118 [in Spanish]. Chilean Ministry of Housing and Urbanism.

MacRae, G., Clifton, G., & Megget, L. (2011). Review of NZ Building Codes of Practice, (August), 1–59. Retrieved from http://canterbury.royalcommission.govt.nz/documents-by-key/20110923.14/$File/ENG.ACA.0016.pdf

Massone, L. M., Bonelli, P., Dragovich, J., Lagos, R., Lüders, C., Moehle, J., & Wallace, J. W. (2012). Seismic Design and Construction Practices for RC Structural Wall Buildings. *Earthquake Spectra*, *28*(SUPPL.1). https://doi.org/10.1193/1.4000047

Rodriguez, E. M., Botero, J. C., & Villa, J. (1999). Cyclic Stress-Strain Behavior of Reinforcing Steel Including Effect of Buckling. *Journal of Structural Engineering*, *125*(6), 605–612.

Standards New Zealand. (2004). *NZS 1170.5:2004: Structural Design Actions Part 5: Earthquake actions - New Zealand*. Wellington: Standards New Zealand.

Standards New Zealand. (2012). *NZS 3101:2006 Concrete Structures Standard Part 1 - The Design of Concrete Structures (Amendment 2)*. Wellington, New Zealand.

Standards New Zealand. (2015). Draft Number: DZ 3101:2006 Amendment 3 – Part 1 Public Comment Draft. Wellington, New Zealand: Standards New Zealand.

Stevenson, C., Smith, A., van Ballegooy, R., & Weng, K. Y. (2015). Personal communication., Sept. 2015. Auckland, New Zealand.

Whitman, Z. J. (2015). *Investigation of Seismic Failure Modes in Flexural Concrete Walls Using Finite Element Analysis*. The University of Washington.

Yong, P. (2016). Personal Communication, March 2016. Auckland, New Zealand.

Yoshimura, M., Kurose, Y., & Wight, J. K. (ed). (1985). Earthquake Effects on Reinforced Concrete Structures: Inelastic Behavior of the Building. *American Concrete Institute*, *SP84*, 163–175.